Accepted Manuscript

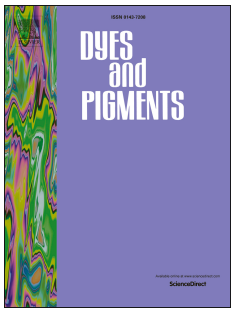

Aggregated-induced Emission Phenothiazine Probe for Selective Ratiometric Response of Hypochlorite Over Other Reactive Oxygen Species

Linlin Wang, Yue Hu, Yi Qu, Jingli Xu, Jian Cao

PII: S0143-7208(16)00021-8

DOI: 10.1016/j.dyepig.2016.01.010

Reference: DYPI 5063

To appear in: *Dyes and Pigments*

Received Date: 23 November 2015

Revised Date: 7 January 2016

Accepted Date: 8 January 2016

Please cite this article as: Wang L, Hu Y, Qu Y, Xu J, Cao J, Aggregated-induced Emission Phenothiazine Probe for Selective Ratiometric Response of Hypochlorite Over Other Reactive Oxygen Species, *Dyes and Pigments* (2016), doi: 10.1016/j.dyepig.2016.01.010.

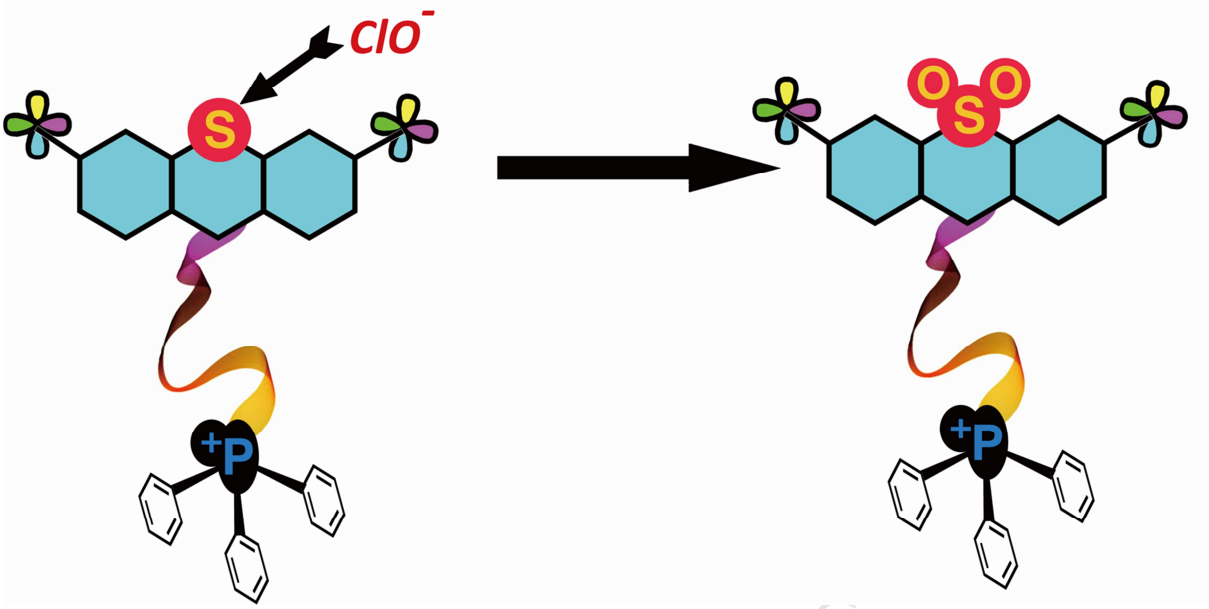

Aggregated-induced Emission Phenothiazine Probe for Selective Ratiometric Response of Hypochlorite Over Other Reactive Oxygen Species

Linlin Wang, Yue Hu, Yi Qu*, Jingli Xu and Jian Cao*

School of Chemistry and Chemical Engineering, Shanghai University of Engineering Science, 333 Longteng Road, Shanghai, 201620, PR China. Fax: 86-21-67791214. E-mail: caoj@sues.edu.cn; quyi@fudan.edu.cn

Abstract

In order to perform a ratiometric fluorescent sensor to recognize hypochlorite over other reaction oxidation species, a simple phenothiazine probe (**QC1**) with double dioxaborolane moieties was designed and synthesized. **QC1** provided blue emission in aqueous and solid state. Double dioxaborolane and quaternary phosphonium salt was introduced into the molecule to prevent aggregation. The sulphur atom at the centre of phenothiazine was to respond to the hypochlorite at room temperature over other ROS because of its stronger oxidized ability. **QC1** gave good linear fitting in the ratiometric mode under both absorption and emission titration experiments. Moreover, **QC1** showed lower detection limited that reached 0.95 μM in absorption titration and 0.41 μM in fluorescent titration process.

Keywords: fluorescent probe, ratiometric, phenothiazine, aggregated-induced emission, hypochlorite

1. Introduction

Reactive oxygen species (ROS) plays an indispensable role in a wide variety of biological processes [1-4]. For example, recent studies reported that cancer cells constantly generate high levels of intracellular ROS, due to oncogenic transformation [5]. Among the various ROS, hypochlorous acid (HClO) is a powerful microbicidal agent in the innate immune system for its strong oxidizing property. The endogenous HClO released by the neutrophil plays a vital role in killing a wide range of pathogens [6, 7]. As a result, excessive generation of HClO always implicates in many human diseases, and can be found as inflammation-associated tissue injury [8-12]. Moreover, it is considered that HClO contributes to cardiovascular disease, and cell apoptosis through calcium dependent calpain activation. Therefore, there is urgent need to sense the various biological effects of HClO with lower detection limit, good selectivity and in real time [13, 14].

With high sensitivity and adjustable structure, many small molecular fluorescent sensors were reported, such as cyanide dyes, fluorescein, rhodamine, BODIPY, naphthalimide, Dicyanomethylene-4H-pyran, and so on [15-27]. There are still some challenges to optimize the small molecular fluorescent sensors for HClO: 1) some commercial dyes show poor stability for oxidants. For example, the cyanide dyes are always bleached by ROS [28]; 2) the ratiometric response probe with different fluorescent channels is still not common [29-32].

To solve such problems, it is needed to develop stabile fluorophores and the useful redox reactions that can output the ratiometric signals for sensing HClO

beyond other ROS. In 1985, Brubaker *et. al.* reported a desulfurization technology with NaClO [33]. As we know, one component of the organic sulphur in coal is dibenzothiophene, an analogy of phenothiazine. Further research on the oxidation of phenothiazine indicated the Chlorite can oxidize the dye to sulfones under stronger oxidizing conditions such as the presence of fuming nitric acid and hydrogen peroxide [34]. Based on this knowledge, we hypothesize that the modified phenothiazine can only be oxidized by a strong oxidant, like ClO^-, and we designed the phenothiazine-based fluorescent sensor (**QC1**) to detect ClO^-. As shown in Scheme 1, we introduced two dioxaborolane moieties to enhance the steric of phenothiazine that can restrain π-π stacking of the rigidity dyes. The quaternary phosphonium salt attached on the N atom of phenothiazine also showed steric hindrance effect for the sensor.

<Scheme 1>

2. EXPERIMENTAL

2.1 Materials and instruments

All reagents and solvents were used as received without further purification. Deionized water was used in the experiments throughout. Silica gel (100-200 mesh) was used for column chromatography. Mass determination was made on a GC-TOF MS spectrometry. NMR spectra were recorded on a Varian 400 MHz with chemical shifts reported as ppm (in DMSO-*d6* or $CDCl_3$, TMS as internal standard). Fluorescence measurements were performed on a FS-5 spectrophotometer (Edinburgh, Britain) and the slit width was set as 1 nm for excitation and emission, respectively.

Absorption spectrum was measured on a SHIMADZU UV-3600 spectrophotometer. NO and ClO^- were produced from the dissolution of NOC13 [1-Hydroxy-2-oxo-3-(3-aminopropyl)-3-methyl-1-triazene][35] and NaClO in the de-ion water, respectively. H_2O_2 was diluted from the stabilized 30% H_2O_2 solution. Hydroxyl radical (·OH) was generated by reaction of 1mM Fe^{2+} with 200μM H_2O_2. Tert-butoxy (t-BuOO·) was prepared from the reaction of 1mM Fe^{2+} with 200μM TBHP. $NaNO_3$ and $NaNO_2$ were used as the source of NO_3^- and NO_2^-, respectively.

2.2 Synthesis of QC1

<Scheme 2>

2.2.1 Synthesis of compound **2**

Compound **1** (180 mg, 0.5 mmol), bis(pinacolato)diboron (254 mg, 1.0 mmol), Pd(dppf)Cl_2 (36 mg, 0.05 mmol), and sodium acetate (287 mg, 3.5 mmol), were added to a dry Schlenk tube. Then 5 mL of dry DMF was added via syringe and the mixture was stirred under nitrogen at 80 °C for 2 hours. After cooling to room temperature, the mixture was extracted with dichloromethane, washed with water, and the solvent was removed under reduced pressure. The crude product was purified by column chromatography (silica gel, petroleum ether/dichloromethane, 1/5, v/v) to give a light yellow solid (215 mg, 70.0%). ^{1}H NMR (400 MHz, $CDCl_3$) δ (ppm) 7.50 - 7.65 (m, 4 H), 6.83 (d, *J*=8.03 Hz, 2 H), 3.90 (br. s., 2 H), 3.38 (t, *J*=6.78 Hz, 2 H), 1.76 - 1.88 (m, 4 H), 1.46 (br. s., 4 H), 1.34 (s, 24 H); ^{13}C NMR (100MHz, $CDCl_3$) δ ppm 147.2, 134.0, 133.8, 124.3, 114.8, 83.7, 47.2, 33.7, 32.6, 29.7, 27.7, 25.9, 24.8.

2.2.2 Synthesis of **QC1**

A solution of compound **2** (306 mg, 0.5 mmol) and triphenylphosphine (145 mg, 0.55 mmol) in dry toluene (15 mL) was refluxed under nitrogen. The reaction was monitored by TLC. Upon completion, the solvent was removed under reduced pressure. The residue was purified by recrystallization to afford **QC1** (372 mg, 85% yield) as a light yellow solid. ^{1}H NMR (400 MHz, $CDCl_3$) δ (ppm) 7.68 - 7.82 (m, 15 H), 7.54 - 7.63 (m, 2 H), 7.47 (s, 2 H), 6.75-6.90 (m, 2 H), 3.87 (br. s., 2 H), 3.53 - 3.66 (m, 2 H), 1.69 (br. s., 2 H), 1.59 (s, 4 H), 1.39-1.46 (m, 2 H), 1.32 (s, 24 H); ^{13}C NMR (100MHz, $CDCl_3$) δ (ppm) 147.28, 135.02, 134.21, 133.66, 133.56, 130.60, 130.48, 124.10, 118.64, 117.79, 115.20, 83.73, 46.84, 29.40, 25.90, 25.73, 24.84, 22.81, 22.30. HRMS(ESI): Found: $[M-Br]^-$ 796.3917; requires $[M-Br]^-$ 796.3927 .

2.2.3 Synthesis of compound **3**

Sodium hypochlorite solution (7.0 %, 2 mL) was added dropwise to a solution of phenothiazine (199 mg, 1 mmol) in acetic acid (10 mL) was stirred at 90 °C overnight. After cooled down, the water was added and extracted with ethyl acetate. The separated organic layer was and washed with water and brine, then dried over Na_2SO_4 and removed under reduced pressure. The crude product was purified by column chromatography (silica gel, petroleum ether/ ethyl acetate, 1/4, v/v) to afford 180 mg (78%) of 3 as a pale brown solid. ^{1}H NMR (400MHz, DMSO-*d6*) δ (ppm) 10.91 (s, 1 H), 7.92 (d, *J* = 8.0 Hz, 2 H), 7.65 (t, *J* = 7.8 Hz, 2 H), 7.35 (d, *J* = 8.3 Hz, 2 H), 7.25 (t, *J* = 7.7 Hz, 2 H); ^{13}C NMR (100MHz, DMSO-*d6*) δ (ppm) 138.61, 133.75, 122.91, 121.91, 121.11, 117.46.

3. Results and Discussion

3.1 Synthesis and characteristic

The synthetic route to **QC1** is illustrated in Scheme 2. Precursor **1** was synthesized by alkylation reaction based on S_N mechanism according to previously published report [36-38]. Two boronic acid esters were introduced by palladium catalysed cross coupling reactions with bis(2,4-dimethylpentane-2,4-glycolato)diboron as boron source. $Pd(dppf)_2Cl_2$ was chosen as the palladium catalyst. Triphenylphosphine (**TPP**) group was attached on the end of the side chain through the one-pot reaction of the toluene solution of **2** and 1.1 equiv. of Ph_3P under the reflux condition.

Fig. 1 shows the imperceptible changes on the structure of the probe and its precursors (**2** and **TPP**) by ^1H and ^{13}C NMR techniques. Firstly, we used ^1H NMR to study the migration of the methylene and phenyl groups. As shown in Fig. 1A, the -CH_2- and phenyls attached on the $\mathbf{P^+}$ migrated from 3.38 and 7.38 to 3.58 and 7.73, respectively. The ^{13}C NMR spectra can directly discover the slight variations in the structure. The alkyl carbon and the phenyl carbon directly attached on the $\mathbf{P^+}$ moved to 22 ppm and 120 ppm, respectively.

<Fig. 1>

3.2 Photophysical properties of QC1

3.2.1 Photophysical properties of **QC1** in solid state and different solvents

QC1 showed distinct blue emission at solid state (Inset in Fig. 2A). Its

absorption and emission spectra were shown in Fig. 2A. The absorption and emission peaks of **QC1** located at 403 and 485 nm, respectively. Then, the fluorescent property was also explored in the solutions. When excited at 400 nm, the maximum emission bands of **QC1** varied from 430 nm to 482 nm in different solvents.

<Fig. 2>

3.2.2 Aggregated-induced Emission (AIE) property of **QC1**

AIE effect was first reported by Prof. Tang in 2001[39]. Here, we found that **QC1** can also work as the AIEgen[40, 41]. The emission property of **QC1** was investigated in DMSO-water mixture to prove its AIE characters (Fig. 3). In pure DMSO solution, **QC1** had very low emission intensity (Φ_f < 0.01). The emission intensity of **QC1** enhanced quickly with increasing fraction of water from 10% to 70%. Furthermore, the intensity was decreased for the stability of **QC1** in the aqueous. However, the about 2000-fold enhancement indicates the potential application of **QC1** for ROS detection in water phase.

< Fig. 3>

3.3 Sensing of QC1 for ClO^-

3.3.1 Sensitivity of **QC1**

The sensing ability of **QC1** for ClO^- was investigated by both UV−vis absorption and emission spectroscopies. In the UV−vis absorption spectrum, the **QC1** showed a weak visible band with the absorption wavelength at 313 nm and the strong absorbance at 269 nm (Fig. 4a). Upon addition of ClO^-, the absorption peak around 313 nm was up, and the absorption peak around 269 nm was down. A linear fitting

was obtained from 0 to 20 μM range implying that **QC1** can work as the colorimetric probe for detecting ClO^- in ratiometric method (Fig. 4b).

Compared with the uncolored UV-vis detection method, the bright blue emission of **QC1** indicated the practical application in fluorescent probe. As shown in Fig. 4c, with gradual addition of ClO^- the emission peak at 381 nm turned on and the one at 486 nm was shutdown. Highly sensitive response was found in the range of 0 to 10 μM indicating that **QC1** is more suitable in the fluorescent method than the colorimetric method. The 3δ/k method was used to evaluate the detection limited (DL) of **QC1**. As shown in Fig. S1, the DL value of **QC1** reached 0.95 μM and 0.41 μM in UV-vis and fluorescence approaches.

< Fig. 4>

< Fig. 5>

The quantum yields of QC1 was tested in aqueous and with the quinoline sulfate (Φ=0.5) as a reference. The measured fluorescence quantum efficiency of QC1 is 0.21 in aggregated state and 0.48 in THF solution.

3.3.2 Mechanism of **QC1** reacted with ClO^-

To verify the recognizing process of **QC1** through the oxidant sulphur atom pathway, we used ^1H NMR titration experiments to spy the changes on the probe. As shown in Fig. 5a, **QC1** had broad bands were located at around 6.82 ppm and 7.6 ppm (marked with the blue areas), the same with phenothiazine (Fig. S2a).

When 1 eq. of NaClO was added, both broad bands transformed to double bands at the same locations (marked with the orange areas in Fig. 5b). Furthermore, we added 100 eq. H_2O_2 to the **QC1** sample and incubated it at 50 ^oC for 10 min. Then, the same spectrum was obtained in Fig. 5c. According to the previous reports, the product of **QC1** oxidized by NaClO coincided with the one oxidized by H_2O_2. We also tested the ^1H NMR spectrum of phenothiazine and NaClO. In Fig. S2b, the broad bands of phenothiazine transformed to the double bands liked **QC1**, which again supported the mechanism. On the contrary, this phenomenon was not found in the titration process of (4-iodobutyl)triphenylphosphonium iodide (Fig. S3). Additional, consideration of the strong signal at aryl region from the bulk triphenylphosphine group, we chose the original phenothiazine dye for a control experiment. As shown in Fig. S4, the oxide of phenothiazine showed the characteristic peak at lower field around 7.0 ~ 8.0 ppm than the unoxidized dye.

3.3.3 Selectivity of **QC1**

Selectivity was another important parameter for a fluorescent probe. We applied different ROS to evaluate the reaction activity of **QC1**. As shown in Fig. 6, the maximum response of the emission intensity ratio at 381 nm and 482 nm reached 10.3 when 1 eq. of ClO^- was added in the system. The ratio value were lower than 5 when other ROS added, such as H_2O_2, *t*-BuOOH etc. The Fe^{2+} caused tiny variation which was used to produce free radicals like the hydroxyl free radical.

< Fig. 6>

4. Conclusion

In summary, we have developed a new phenothiazine based on AIE gen (**QC1**) that can be used as a ratiometric fluorescent detector for probing ClO^- over other common ROS species in HEPES buffer. Strong fluorescent signals obtained in solid state (over 2000-fold than in DMSO) indicated this probe can be widely used in the field of sensors. The high sensitivity of **QC1** was recorded by titration experiment (0~3 eq. of ClO^-) and the calculation of detection limited value (3δ/k method, 0.41 μM). A new detecting process for ClO^- was performed based on the fast reaction between ClO^- and phenothiazine. We believe that it can support a series of ClO^--SENSORS with highly specific. Furthermore, we are working on modifying the emission wavelength on the phenothiazine dyes.

Acknowledgements

This work was supported by NSFC/China (21404068), Talent Program of Shanghai Municipal Education Commission (ZZGCD15029) and Shanghai University of Engineering Science (A1-5300-14-020303, A1-5300-15-010228 and E1-0501-15-0113). We thank Professor Zhihua Sun and his group for kindly helping with organic synthesis site and recording of NMR spectra.

References

[1] Que EL, Domaille DW, Chang CJ. Metals in neurobiology: probing their chemistry and biology with molecular imaging. Chem Rev 2008; 108: 1517—1549.

[2] D'Autreaux B, Toledano MB. ROS as signalling molecules: mechanisms that generate specificity in ROS homeostasis. Nat Rev Mol Cell Biol 2007; 8: 813－824.

[3] Xu K, Wang L, Qiang M, Wang L, Li P, Tang B. A selective near-infrared fluorescent probe for singlet oxygen in living cells. Chem Commun 2011; 47: 7386－7388.

[4] Valko M, Leibfritz D, Moncol J, Cronin MTD, Mazur M, Telser J. Free radicals and antioxidants in normal physiological functions and human disease. Int J Biochem Cell Biol 2007; 39: 44－84.

[5] Shim M, Xia Y. A reactive oxygen species (ROS)-responsive polymer for safe, efficient, and targeted gene delivery in cancer cells. Angew Chem Int Ed 2013; 52: 6926－6929.

[6] Shepherd J, Hilderbrand SA, Waterman P, Heinecke JW, Weissleder R, Libby P. A fluorescent probe for the detection of myeloperoxidase activity in atherosclerosis-associated macrophages. Chem Biol 2007; 14: 1221－1231.

[7] Harrison JE, Schultz J. Studies on the chlorinating activity of myeloperoxidase. J Biol Chem 1976; 251: 1371－1374.

[8] Yap YW, Whiteman M, Cheung NS. Chlorinative stress: an under appreciated mediator of neurodegeneration. Cell Signal 2007; 19: 219－228.

[9] Suzuki T. DNA damage and mutation caused by vital biomolecules, water, nitric oxide, and hypochlorous acid. Genes Environ 2006; 28: 48－55.

[10] Perez-Vilar J, Boucher RC. Reevaluating gel-forming mucins' roles in cystic

fibrosis lung disease. Free Radical Biol Med 2004; 37: 1564－1577.

[11] Rao RK. Oxidative stress-induced disruption of epithelial and endothelial tight junctions. Front Biosci 2008; 13: 7210－7226.

[12] Que EL, Domaille DW, Chang CJ. Metals in neurobiology: probing their chemistry and biology with molecular imaging. Chem Rev 2008; 108: 1517－1549.

[13] Pattison DI, Davies MJ. Kinetic analysis of the role of histidine chloramines in hypochlorous acid mediated protein oxidation. Biochemistry 2005; 44: 7378－7387.

[14] Chen XQ, Tian X, Shin I, Yoon, J. Fluorescent and luminescent probes for detection of reactive oxygen and nitrogen species. Chem Soc Rev, 2011; 40: 4783－4804.

[15] De Silva AP, Gunaratne HQN, Gunnlaugsson T, Huxley AJM, McCoy CP, Rademacher JT, Rice TE. Signaling recognition events with fluorescent sensors and switches. Chem Rev 1997; 97: 1515－1566.

[16] Vendrell M, Zhai, D, Er, JC, Chang Y-T. Combinatorial strategies in fluorescent probe development. Chem Rev 2012; 112: 4391－4420.

[17] Yang Y, Zhao Q, Feng W, Li F. Luminescent chemodosimeters for bioimaging. Chem Rev 2013; 113: 192－270.

[18] Xu QL, Heo CH, Kim G, Lee HW, Kim HM, Yoon J. Development of imidazoline-2-thiones based two-photon fluorescence probes for imaging hypochlorite generation in a co-culture system. Angew Chem Int Ed 2015; 54:

4890－4894.

[19] Shi CX, Guo ZQ, Yan YL, Zhu SQ, Xie YS, ZhaoYS, Zhu WH, Tian H. Self-assembly solid-state enhanced red emission of quinolinemalononitrile: optical waveguides and stimuli response. ACS Appl Mater Interfaces 2013; 5: 192－198.

[20] Wu XM, Sun XR, Guo ZQ, Tang JB, Shen YQ, James TD, Tian H, Zhu WH. In vivo and in situ tracking cancer chemotherapy by highly photostable NIR fluorescent theranostic prodrug. J Am Chem Soc 2014; 136: 3579－3588.

[21] Yuan L, Lin W, Yang Y, Chen H. A unique class of near-infrared functional fluorescent dyes with carboxylic-acid-modulated fluorescence ON/OFF switching: rational design, synthesis, optical properties, theoretical calculations, and applications for fluorescence imaging in living animals. J Am Chem Soc 2012; 134: 1200－1211.

[22] Pluth MD, Tomat E, Lippard SJ. Biochemistry of mobile zinc and nitric oxide revealed byfluorescent sensors. Annu Rev Biochem 2011; 80: 333－355.

[23] Cheng GH, Fan JL, Sun W, Sui K, Jin X, Wang JY, Peng XJ. A highly specific BODIPY-based probe localized in mitochondria for HClO imaging. Analyst 2013; 138: 6091－6096.

[24] Liu F, Wu T, Cao JF, Zhang H, Hu MM, Sun SG, Song FL, Fan JL, Wang JY, Peng XJ. A novel fluorescent sensor for detection of highly reactive oxygen species, and for imaging such endogenous hROS in the mitochondria of living cells. Analyst 2013; 138: 775－778.

[25] Chen GW, FL, Wang JY, Yang ZG, Sun SG, Fan JL, Qiang XX, Wang X, Doub BR, Peng XJ. FRET spectral unmixing: a ratiometric fluorescent nanoprobe for hypochlorite. Chem Commun 2012; 48: 2949－2951.

[26] Lou XD, Zhang Y, Li QQ, Qin JG, Li Z. A highly specific rhodamine-based colorimetric probe for hypochlorites: a new sensing strategy and real application in tap water. Chem Commun 2011; 47: 3189－3191.

[27] Yu FB, Li P, Song P, Wang BS, Zhao JZ, Han KL. Facilitative functionalization of cyanine dye by an on‐off‐on fluorescent switch for imaging of H2O2 oxidative stress and thiols reducing repair in cells and tissues. Chem Commun 2012; 48: 4980－4982.

[28] Oushiki D, Kojima H, Terai T, Arita M, Hanaoka K, Urano Y, Nagano T. Development and application of a near-infrared fluorescence probe for oxidative stress based on differential reactivity of linked cyanine dyes. J Am Chem Soc 2010; 132: 2795－2801.

[29] Guo T, Cui L, Shen JN, Wang R, Zhu WP, Xu YF, Qian XH. A dual-emission and large Stokes shift fluorescence probe for real-time discrimination of ROS/RNS and imaging in live cells. Chem Commun 2013; 49: 1862－1864.

[30] Koide Y, Urano Y, Kenmoku S, Kojima H, Nagano T. Design and synthesis of fluorescent probes for selective detection of highly reactive oxygen species in mitochondria of living cells. J Am Chem Soc 2007; 129: 10324－10325.

[31] Panizzi P, Nahrendorf M, Wildgruber M, Waterman P, Figueiredo JL, Aikawa E, McCarthy J, Weissleder R, Hilderbrand SA. Oxazine conjugated nanoparticle

detects in vivo hypochlorous acid and peroxynitrite generation. J Am Chem Soc 2009; 131: 15739－15744.

[32] Setsukinai K, Urano Y, Kakinuma K, Majima HJ, Nagano T. Development of novel fluorescence probes that can reliably detect reactive oxygen species and distinguish specific species. J Biol Chem 2003; 278: 3170－3175.

[33] Brubaker RB, Stoicos T. Precombustion coal desulfurization with sodium hypochlorite. In processing and utilization of high sulfur coals; Attia, YA. Proceedings of the first international conference on processing and utilization of high sulfur coals, October 13－17, 1985, Columbus, OH; Elsevier: New York, 1985; pp 311－326.

[34] Jonnalagadda SB, Pare BK. Oxidation of toluidine blue by chlorite in acid and mechanisms of the uncatalyzed and Ru(III)-catalyzed reactions: a kinetic approach. J Phys Chem A 2010, 114: 12162－12167vg.

[35] Joseph A. Hrabie, John R. Klose, David A. Wink, Keefer LK. New nitric oxide-releasing zwitterions derived from polyamines. The Journal of Organic Chemistry 1993; 58: 1472－1476.

[36] Qu Y, Hua HL, Tian H. Colorimetric and ratiometric red fluorescent chemosensor for fluoride ion based on diketopyrrolopyrrole. Org Lett 2010; 12: 3320－3323.

[37] Qu Y, Yang JB, Hua JL. Thiocarbonyl quinacridone-based “turn on” fluorescent chemodosimeters for highly sensitive and selective detection of Hg(II). Sensor Actuat B: Chem 2012; 161: 661－668.

[38] Deng L, Wu WT, Guo HM, Zhao JZ, Ji SM, Zhang X, Yuan XL, Zhang CL.

Colorimetric and ratiometric fluorescent chemosensor based on diketopyrrolopyrrole (DPP) for selective detection of thiols: an experimental and theoretical study. J Org Chem 2011; 76: 9294－9304.

[39] Luo JD, Xie ZL, Lam JWY, Cheng L, Chen HY, Qiu CF, Kwok HS, Zhan XW, Liu YQ, Zhu DB, Tang BZ. Aggregation-induced emission of 1-methyl-1,1,3,4,5 - pentaphenylsilole. Chem Commun 2001; 1740－1741.

[40] Zhang X, Zhang X, Yang B, Liu M, Liu W, Chen Y, Wei Y. Polymerizable aggregation-induced emission dye-based fluorescent nanoparticles for cell imaging applications. Polym Chem. 2014; 5: 356－360.

[41] Zhang X, Zhang X, Yang B, Hui J, Liu M, Chi Z, Liu S, Xu J, Wei Y. A novel method for preparing AIE dye based cross-linked fluorescent polymeric nanoparticles for cell imaging. Polym Chem. 2014; 5: 683－688.

Scheme and Figure Captions:

Scheme1. The descript of probe QC1 and its recognition mechanism towards NaClO.

Scheme 2. Synthesis Routine of probe **QC1**.

Fig. 1. ^{1}H and ^{13}C NMR spectra of probe **QC1** and its precursors.

Fig. 2. (A) PL spectra of the **QC1** in solid state. λ_{ex}: 400 nm. (B) Normalized emission spectra of **QC1** in different solvents. λ_{ex}: 400 nm. (Inset in Fig. 2A: solid fluorescence of **QC1**)

Fig. 3. (A) Aggregated-induced emission spectra of **QC1** performed in DMSO system with different fraction of water (0~99%); (B) Emission enhancement of **QC1** towards different fraction of water.

Fig. 4. (A) Changes in the absorption spectra of **QC1** (10 μM) upon ClO^- addition in HEPES (pH = 7.4, contained 1% DMSO); (B) ratio of absorbance at 312 nm and 269nm with the addition of ClO^-; (C) Changes in the emission spectra of **QC1** (10 μM) upon ClO^- addition in HEPES (pH = 7.4, contained 1% DMSO); (D) ratio of fluorescent intensity at 381 nm and 482 nm with the addition of ClO^-.

Fig. 5. ^{1}H NMR titration of **QC1** with 0 eq. (A), 1 eq. NaClO (B) and 100 eq. H_2O_2(C).

Fig. 6. Various ROS species selectivity profiles of **QC1** (10 μM) in the presence of various ROS species in HEPES (pH = 7.2, contained 1% DMSO).

Scheme-1

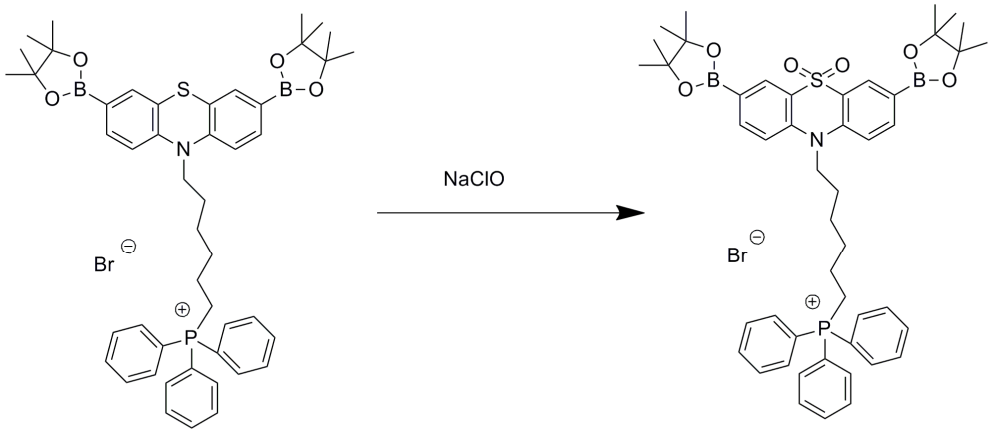

QC1

Scheme-2

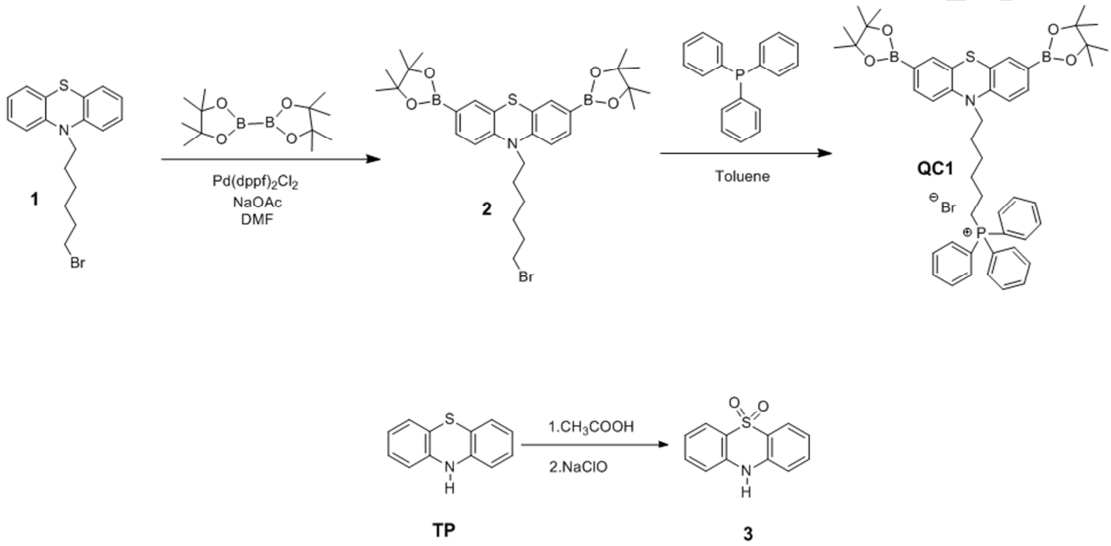

Figure-1

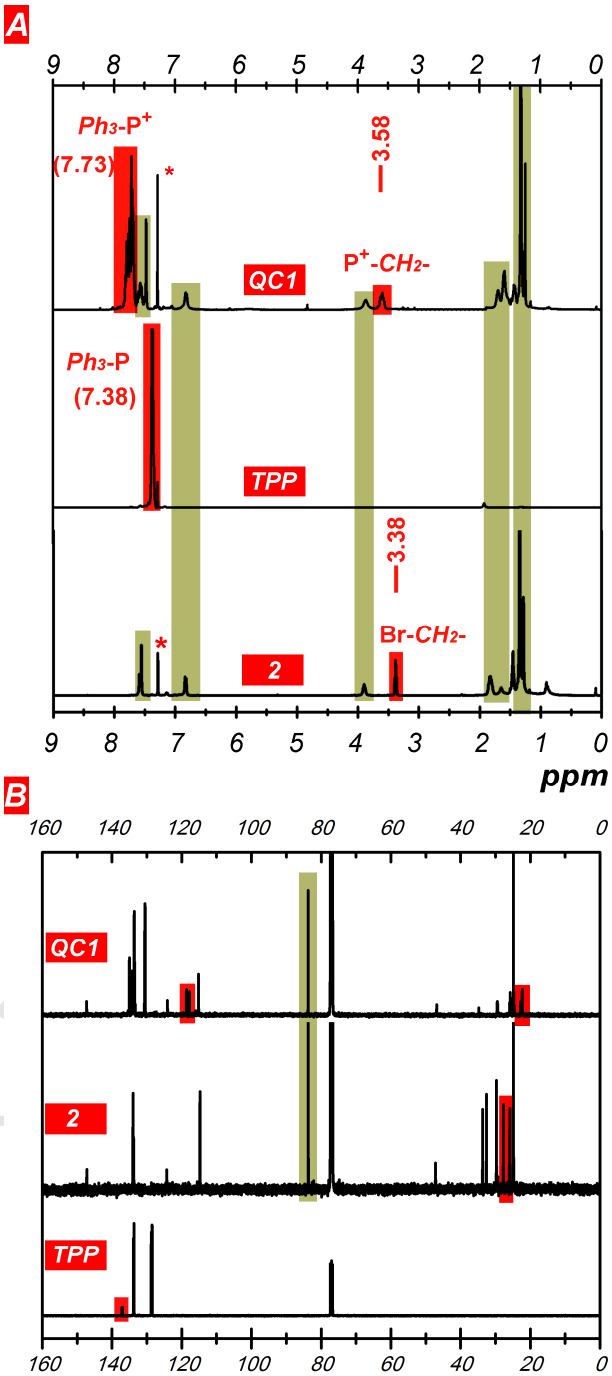
A
9 8 7 6 5 4 3 2 1 0
Ph3-P+
(7.73)
*
3.58
QC1
P+-CH2-
Ph3-P
(7.38)
TPP
3.38
Br-CH2-
*
2
9 8 7 6 5 4 3 2 1 0
ppm
B
160 140 120 100 80 60 40 20 0
QC1
2
TPP
160 140 120 100 80 60 40 20 0

Figure-2

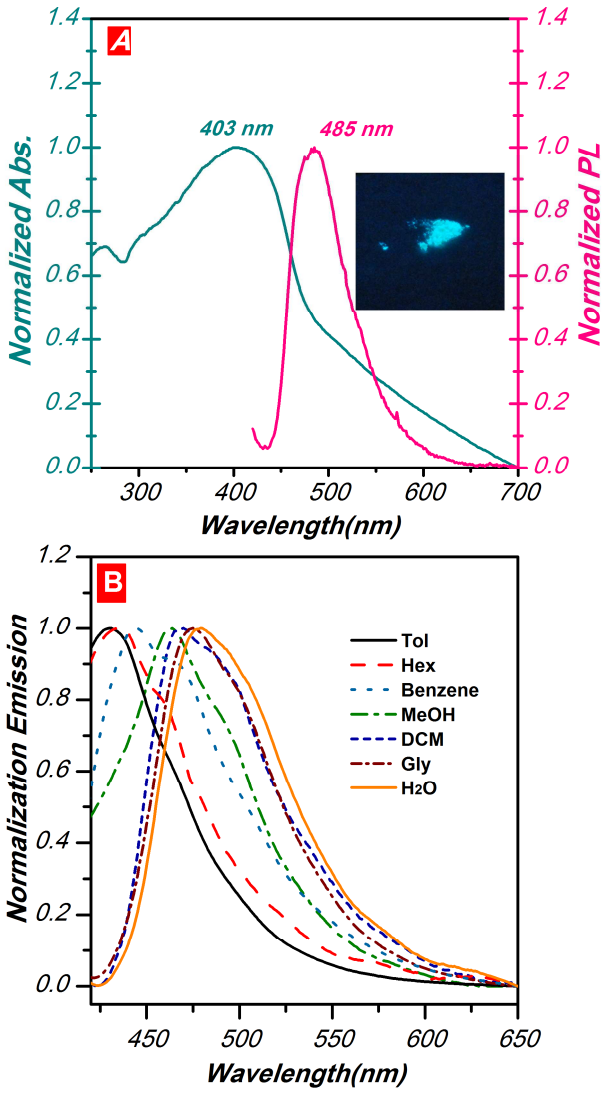
A
403 nm
485 nm
Normalized Abs.
Normalized PL
Wavelength(nm)
B
Tol
Hex
Benzene
MeOH
DCM
Gly
H2O
Normalization Emission
Wavelength(nm)

Figure-3

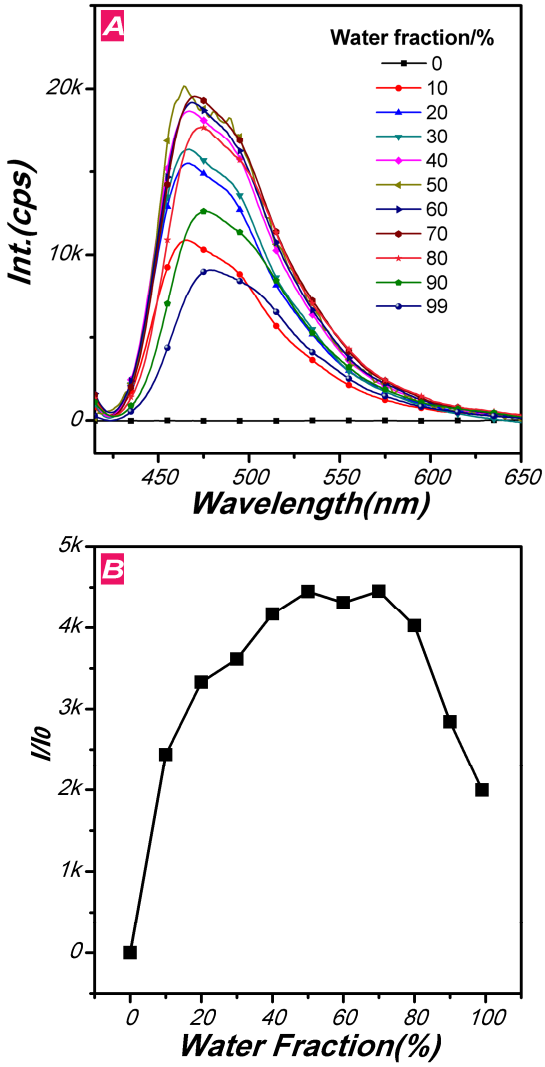
A
Water fraction/%
0
10
20
30
40
50
60
70
80
90
99
Int.(cps)
20k
10k
0
450
500
550
600
650
Wavelength(nm)
B
I/I0
5k
4k
3k
2k
1k
0
0
20
40
60
80
100
Water Fraction(%)

Figure-4

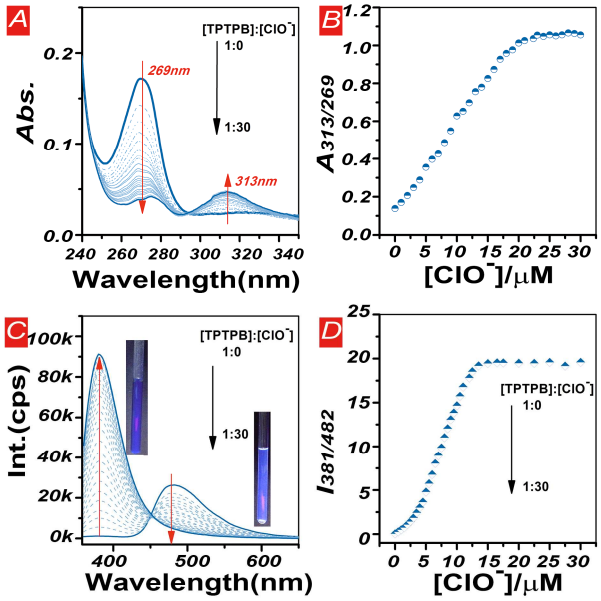

Figure-5

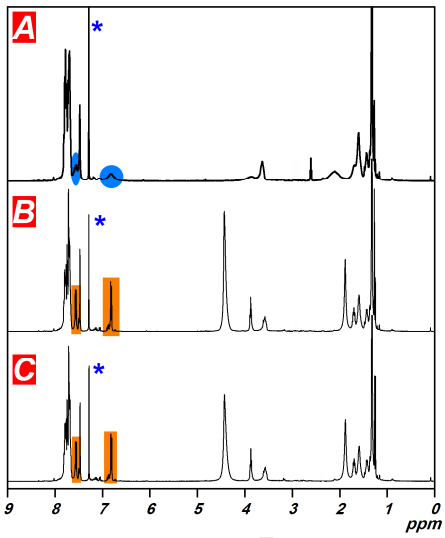

Figure-6

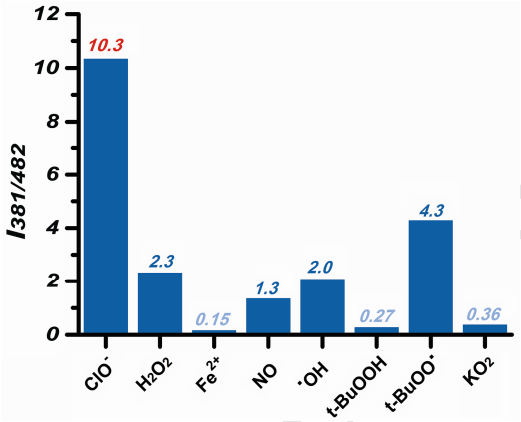

1. A phenothiazine probe (**QC1**) with double dioxaborolane moieties was designed and synthesized.

2. A stability phenothiazine was chosen as the report unit to avoid oxidant bleaching process.

3. The fluorescent sensor (**QC1**) was designed for detecting ClO^-.

4. A new reaction and ratiometric signals for sensing HClO beyond other ROS.

5. **QC1** showed lower detection limited in absorption and fluorescent titration process.